5. Ya. B. Zel'dovich and Yu. P. Raizer, The Physics of Shock Waves and High-Temperature Hydrodynamic Pressures [in Russian], Nauka, Moscow (1966).

A METHOD FOR INVESTIGATING MATERIAL PROPERTIES DURING DYNAMIC ELONGATION

B. I. Abashkin, I. Kh. Zabirov, V. S. Lobanov, and V. G. Rusin

UDC 620.178.3/7

In the high-speed impact of flat plates tensile stresses arising as a result of the interaction of incident waves and waves reflected from contact and free surfaces can lead to scab fracture. The direct experimental measurement of the critical stress and the corresponding strain in the scabbing zone is very difficult, and therefore these quantities are estimated by starting from various indirect measurements and making certain assumptions about the behavior of the material under elongation at a high strain rate. This problem is treated in a number of papers [1-8] in which scab fractures are studied experimentally and analytically. A detailed bibliography of this problem is given in [1, 7, 8]. These papers are characterized by the use of an elastic model of the material in determining the scab stress. We present an experimental—theoretical method for determining the stress—strain curve of a material clear up to scabbing using the more complicated elastoplastic model of a solid.

The basic equations and relations describing the one-dimensional unsteady motion of a continuous medium are written in the Lagrange—Euler form and are similar to those used in [9, 10].

The equation of motion

$$(1/V)\rho_0 du/dt = \partial\sigma/\partial x, \quad (1)$$

where ρ_0 is the initial density; u is the mass velocity; $-p + s = \sigma$ is the total stress; s is the shear part of the total stress; p is the bulk pressure (the spherical part of the stress tensor); and $\rho_0/\rho = V$ is the compressive strain.

The equation of continuity

$$(1/V)dV/dt = \partial u/\partial x. \quad (2)$$

The energy equation

$$dE/dt - Vsd\varepsilon/dt + pdV/dt = 0, \quad (3)$$

where $\varepsilon = \rho_0/\rho - 1$.

The equation of the stress deviator

$$ds/dt = 2\mu(d\varepsilon/dt - (1/3V)dV/dt), \quad (4)$$

where μ is the Lamé constant.

The rate of strain

$$d\varepsilon/dt = \partial u/\partial x. \quad (5)$$

The equation of state in the Mie—Grüneisen form

$$p_1 = p_H + \rho\Gamma(E - E_H), \quad (6)$$

Moscow. Translated from Zhurnal Prikladnoi Mekhaniki i Tekhnicheskoi Fiziki, No. 4, pp. 109-114, July-August, 1977. Original article submitted June 23, 1976.

where p_H and E_H are the pressure and internal energy on a Hugoniot shock adiabat, and Γ is the Grüneisen coefficient.

The hydrodynamic part of the flow is described by the viscous fluid model. In this case the expression for the pressure is written in the form

$$p = p_1 + Q; \tag{7}$$
$$Q = \eta_1 \partial u/\partial x + (\partial u/\partial x)^2 \eta_2, \tag{8}$$

where η_1 and η_2 are functions of the initial density, the bulk sound speed, and certain dimensionless parameters. The first term in Eq. (8) is the physical Navier–Stokes viscosity, and the second is the artificial von Neumann–Richtmyer viscosity which brings about the spreading of the shock fronts to a finite width.

The plastic state of the medium is described by the equations of the theory of plastic flow. The plasticity condition is chosen in the generalized Mises form

$$I_2' \geqslant K^2, \tag{9}$$

where I_2' is the second invariant of the stress tensor deviator and K is a certain functional of pure shear or simple elongation. The yield surface is the surface of a circular cone in the coordinates of the principal stresses.

The condition for the onset of scabbing is chosen in the form

$$\sigma \geqslant \sigma_*, \tag{10}$$

where σ_* is the tensile strength (scabbing strength).

We take the following fracture criterion: Fracture of a continuous material occurs when the instantaneous tensile stress exceeds a certain characteristic value. Plasticity and scabbing are described by specially developed procedures for correcting the stressed state at a given point. These procedures are described in detail in [9, 10].

Equations (1)-(7) together with conditions (8)-(10) and the appropriate initial and boundary conditions form a closed correctly formulated problem. The initial and boundary conditions are the following: At time t = 0 the striker plate velocity is specified and the external pressure is assumed constant and equal to zero.

Equations (1)-(7) with the boundary and initial conditions indicated above were integrated numerically to the second order of accuracy by using an explicit difference scheme. Problems related to the correctness of the numerical solutions, the choice of an appropriate difference scheme, the analysis of its stability, and other procedural features are discussed in [9]. Figure 1 shows the schematic loading–unloading curve which was used in the calculations. Curve OAB is a shock adiabat, E_1E is the bulk compression and elongation, curve BC is the elastic part of the unloading, curve CD is the plastic part of the unloading in the compression and elongation region, σ_+ is the tensile yield stress, σ_* is the tensile strength, σ_- is the compressive yield stress, O_1O and O_2O are the elastic parts of the pressure, O_1E_1 is the part of the stress–strain curve $p = p(\xi)$ being sought (the spherical part of the stress tensor) in the plastic deformation region. Curve O_1E_1 is given in the form

$$p = p_*[1 - \beta(1 - \xi/\xi_*)^n], \tag{11}$$

where $\xi = \rho/\rho_0 - 1 = -\varepsilon/(1 + \varepsilon)$, $\xi_+ \leqslant \xi \leqslant \xi_*$. The parameters p_*, ξ_*, β, and n are determined from the values of the functions and their derivatives at points O_1 and E_1. At point E_1 the derivative $dp/d\xi = 0$, and at point O_1 the derivative $dp/d\xi$ is the slope of the elastic part of the pressure. The parameters of curve II for a monolayer target are determined from ex-

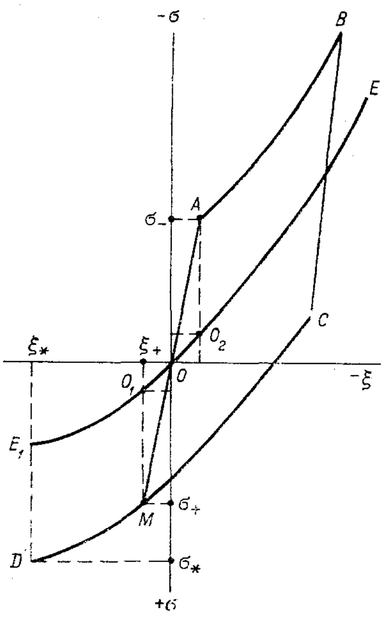

Fig. 1

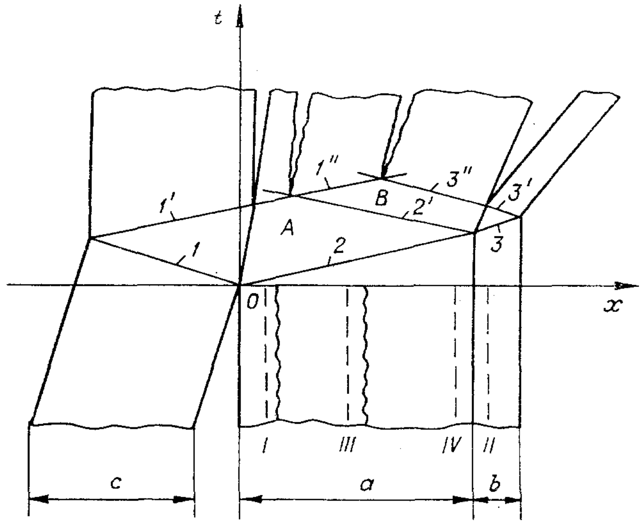

Fig. 2

perimental values of the critical impact velocity and the thickness of the scabbed-off layer. Table 1 lists the calculated values of the coefficients of curve II for AMG-6 and plastic. The experimental procedure is based on well-known methods of slowing down, reflection [11], and artificial scabbing, and is similar to the procedure in [2]. The two-layer target consisted of two plates of different materials having known shock adiabats, with the shock impedance of the second layer smaller than that of the first. Contacting surfaces of the first and second layers are carefully finished and bonded by a thin layer of vacuum oil to ensure their adhesion. The striker and the first layer of the target were made of the material under study. With the geometry chosen for the target and striker a one-dimensional deformation in the central part of the target at least 30 mm in diameter and scab fracture connected exclusively with this deformation were produced. By considering the impact process on a schematic t–x diagram (Fig. 2), where the fine lines denote wave trajectories and the heavy lines trajectories of the free surfaces of the plates and the scab surfaces, sections of possible scab fractures of the first layer of the target can be determined. During impact shock waves 2 and 1 propagate through the first layer of the target *a* and the striker c, respectively. As shock wave 1 leaves the free surface of the striker it is reflected by rarefaction wave 1'. Shock wave 2 in the target is reflected by the wave of partial unloading 2' from the boundary between the target layers, and shock wave 3 enters the second layer. The interaction of rarefaction waves 2' and 1' leads to the creation of tensile stresses in section A. If $\sigma \geqslant \sigma_*$, scab fracture occurs in section A and rarefaction wave 1" is formed. If $\sigma < \sigma_*$, 1" will be a tensile wave. Shock wave 3 in the second layer of the target is reflected from the free surface by rarefaction wave 3'. As the wave leaves the boundary between the target layers the second layer is separated from the first and rarefaction wave 3" is propagated, reducing the stress to zero. The interaction of rarefaction wave 3" with 1" leads to the creation of tensile stresses in section B which for $\sigma \geqslant \sigma_*$ lead to scab fracture.

With the experimental arrangement described above for plane impact of multilayered plates scab fractures of the target can be achieved in one or two sections depending on the impact velocity. We studied two-layer and monolayer targets numerically and experimentally. A monolayer target differing from the two-layer target in the absence of layer b was used to determine the critical impact velocity at which scab fracture first occurs, and in so doing the scabbing section was determined. The values of the critical velocity and the thickness of the scabbed-off layer were used to plot a stress–strain curve and to determine the limiting values of the tensile stress σ_* and the strain ε_*. The experiments and calculations were performed for plastic (ρ_0 = 1.18 g/cm^3, c = 2.68 km/sec) and an aluminum alloy AMG-6 (ρ_0 = 2.65 g/cm^3, c = 5.98 km/sec). The samples of AMG-6 were made from a rod as supplied by the manufacturer. The target and striker were disks 50 mm in diameter, the thickness of the first target layer *a* was 0.5 cm, that of the second layer b was 0.1 cm, and the thickness of the striker c was 0.35 cm. Figure 2 is a schematic diagram of the striker and target; the numbers

TABLE 1

Material	p_*, kbar	ξ_*	n	β
Plastic	−0,7	−0,035	3,25	1,02
AMG-5	−11	−0,022	1,19	1,0

TABLE 2

Material	u, m/sec	Elastoplastic model		Acoustic model	
		σ_*, kbar	ε_*, %	σ_*, kbar	ε_*, %
Plastic	90±3	1,0	3,6	1,42	1,68
AMG-6	230±8	13,0	2,2	18,2	1,92

TABLE 3

Material	Experiment		Calculation	
	u_B, m/sec	u_{AB}, m/sec	u_B, m/sec	u_{AB}, m/sec
AMG-6	230±12	340±15	225±30	340±40

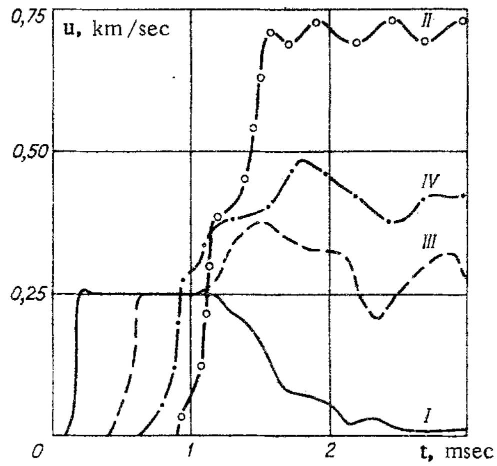

Fig. 3

I-IV denote sections of the target for which the time dependences of the mass velocities calculated numerically are plotted in Fig. 3. The wavy lines (cf. Fig. 2) denote sections in which scab fractures occurred.

Table 2 lists the experimental values of the critical impact velocities, scab stresses, and strains calculated by using the proposed elastoplastic model, and for comparison, the acoustic estimates of these quantities. Table 2 shows that the results obtained with the elastoplastic model differ appreciably from the acoustic approximation.

The main purpose of the experimental and numerical studies with the two-layer target was to test the stress–strain curves II for a more complex wave process, including two scabbings. In this case the striker and the first layer of the target were made of AMG-6 aluminum and the second layer of plastic. The impact velocities at which scab fractures occurred in sections A and B of layer a were calculated and measured. The results of the calculations and experiment (Table 3) showed that as the impact velocity is increased scab fracture occurs first in section B for $u_B \leqslant u \leqslant u_{AB}$; for $u \geqslant u_{AB}$ scabbing occurs in both systems A and B, but in this last case scabbing begins in A earlier than in B. This feature is confirmed qualitatively by considering the impact process on the σ–u diagram. It should be noted that the impact velocity u_B is in good agreement with the critical velocity for a monolayer target in which scabbing occurs in section A. A comparison of the results in Table 3 shows satisfactory agreement of experiment and calculation.

Thus, the results obtained by the method proposed above for calculating dynamic stress–strain curves of materials and checking by special experiments can be used to characterize solutions of problems involving scab fractures.

LITERATURE CITED

1. N. A. Zlatin and B. S. Ioffe, "Time dependence of the resistance to spalling," Zh. Tekh. Fiz., 42, 1740 (1972).
2. B. A. Tarasov, "Quantitative description of spall damage," Zh. Prik. Mekh. Tekh. Fiz., No. 4, 137 (1973).
3. E. V. Menteshev, V. P. Ratnikov, A. P. Rybakov, A. N. Tkachenko, and V. P. Shavkov, "Effect of the explosion of a sheet charge on an aluminum plate," Fiz. Goreniya Vzryva, No. 2 (1967).
4. N. A. Zlatin, S. M. Mochalov, G. S. Pugachev, and A. M. Bragov, "Time relationships of the failure of metals under intensive loading," Fiz. Tverd. Tela, 16, 1752 (1974).
5. V. S. Nikiforovskii, S. I. Sabitova, and A. E. Strelyaev, "Fracture of solid bodies by dynamic loads," Fiz.-Tekh. Probl. Razrab. Polezn. Iskop., No. 5 (1970).
6. A. G. Ivanov, "Scabbing in the acoustic approximation," Fiz. Goreniya Vzryva, No. 3 (1975).
7. L. V. Al'tshuler, "Use of shock waves in high-pressure physics," Usp. Fiz. Nauk, 85, 197 (1965).
8. B. Steverding and A. Werkheiser, J. Mech. Eng. Sci., 13, 200 (1971).
9. V. S. Lobanov, Motion of Certain Continuous Media in an Explosion, Dissertation for Academic Degree of Candidate of Physical and Mathematical Sciences [in Russian], Moscow Physicotechnical Institute (1972).
10. M. L. Wilkins, in: Fundamental Methods in Hydrodynamics, Vol. 3, Academic Press, New York (1964).
11. Ya. B. Zel'dovich and Yu. P. Raizer, Physics of Shock Waves and High-Temperature Hydrodynamic Phenomena, Academic Press, New York (1967).

TENSILE STRESSES IN TARGET UPON COLLISION OF RIGID BODIES

M. S. Kachan and Yu. A. Trishin

UDC 534.211

Introduction. When an explosion occurs in a rigid body, almost half the energy of the explosives passes into the shock wave [1], and therefore shock wave processes play an important part in the breaking up of rocks and metals by impulsive loading. From the physical point of view the process of brittle failure is characterized by the detachment of the material on the free surface under the effect of the tensile stresses in the rock massif or metal plate in case of wave interference [2, 3].

The spalling of a layer of material is investigated in order to reveal its mechanism and the laws governing the process of failure in material under intensive loads ([14, 15] etc.) and to use it in practical problems, e.g., in breaking up rocks [11, 16-18] or for protection at high-speed collision of rigid bodies [19].

In early investigations, in analogy with static loading, the strength upon intensive loading was described by the critical normal breaking stresses σ_*, characteristic for the given material at the stipulated loading conditions [4, 20], and the criterion of failure was adopted in the form

$$\sigma = \sigma_*. \tag{0.1}$$

When a normal tensile stress at any point of the body attained the value σ_*, it was considered the condition leading to failure of the material. This criterion has not lost its importance up to the present [3, 5, 11, 21] because it is a necessary, albeit not sufficient, condition of failure. It was already noted in [20] that spalling is also affected by the shape of the stress wave, and it was assumed that σ_* depends on the conditions of loading and on the stress distribution in the body. Experimental measurements of the resistance to detachment upon spalling, conducted on the same materials by different authors, yielded widely

Novosibirsk. Translated from Zhurnal Prikladnoi Mekhaniki i Tekhnicheskoi Fiziki, No. 4, pp. 114-124, July-August, 1977. Original article submitted July 16, 1976.

 0021-8944/77/1804-0526$07.50